

TABLE OF CONTENTS

Features	1	Maximizing Performance Through Proper Layout	17
Applications.....	1	1/f Noise Characteristics	18
General Description	1	Random Auto-Zero Correction Eliminates Intermodulation Distortion	18
Pin Configurations	1	Broadband and External Resistor Noise Considerations	19
Revision History	3	Output Overdrive Recovery.....	19
Specifications.....	4	Input Overvoltage Protection	19
5 V Electrical Characteristics.....	4	Output Phase Reversal.....	19
2.7 V Electrical Characteristics.....	5	Capacitive Load Drive	20
Absolute Maximum Ratings.....	6	Power-Up Behavior.....	20
Thermal Characteristics	6	Applications Information	21
ESD Caution.....	6	5 V Precision Strain Gage Circuit	21
Typical Performance Characteristics	7	3 V Instrumentation Amplifier	21
Functional Description	15	High Accuracy Thermocouple Amplifier	22
Amplifier Architecture	15	Precision Current Meter.....	22
Basic Auto-Zero Amplifier Theory.....	15	Precision Voltage Comparator.....	22
Auto-Zero Phase.....	16	Outline Dimensions	23
Amplification Phase.....	16	Ordering Guide	25
High Gain, CMRR, and PSRR	17		

REVISION HISTORY**6/15—Rev. E to Rev. F**

Added Patent Note, Note 1.....	1
Change to Input Voltage Parameter, Table 3.....	6
Changes to Ordering Guide.....	25

2/11—Rev. D to Rev. E

Changes to Figure 66	21
Updated Outline Dimensions.....	22
Changes to Ordering Guide.....	23

6/08—Rev. C to Rev. D

Changes to Figure 19 and Figure 20	8
Changes to Figure 44	12
Changes to Figure 38	13
Moved Figure 50 and Figure 51.....	14
Changes to Figure 66, Precision Current Meter Section, Layout, Figure 67, Equation 24, and Figure 68.....	21

5/07—Rev. B to Rev. C

Changes to Features	1
Changes to Table 1	3
Changes to Table 2	4
Changes to Basic Auto-Zero Amplifier Theory Section	14
Changes to Figure 50	15
Changes to Figure 55	16
Changes to Figure 66	21
Updated Outline Dimensions.....	22

9/06—Rev. A to Rev. B

Updated Format	Universal
Changes to Table 1	3
Changes to Table 2	4
Changes to Figure 50	14
Changes to Figure 51	15
Changes to Figure 66	21
Deleted Figure 69 and SPICE Macro-Model Section.....	17
Deleted SPICE Macro-Model for the AD857x Section.....	18
Updated Outline Dimensions.....	22
Changes to Ordering Guide.....	23

7/03—Rev. 0 to Rev. A

Renumbered Figures.....	Universal
Changes to Ordering Guide.....	4
Change to Figure 15.....	16
Updated Outline Dimensions.....	19

10/99—Revision 0: Initial Version

SPECIFICATIONS

5 V ELECTRICAL CHARACTERISTICS

$V_S = 5\text{ V}$, $V_{CM} = 2.5\text{ V}$, $V_O = 2.5\text{ V}$, $T_A = 25^\circ\text{C}$, unless otherwise noted.

Table 1.

Parameter	Symbol	Conditions	Min	Typ	Max	Unit
INPUT CHARACTERISTICS						
Offset Voltage	V_{OS}	$-40^\circ\text{C} \leq T_A \leq +125^\circ\text{C}$		1	5	μV
					10	μV
Input Bias Current	I_B	$-40^\circ\text{C} \leq T_A \leq +125^\circ\text{C}$		10	50	pA
AD8571/AD8574		$-40^\circ\text{C} \leq T_A \leq +125^\circ\text{C}$		1.0	1.5	nA
AD8572		$-40^\circ\text{C} \leq T_A \leq +85^\circ\text{C}$		160	300	pA
		$-40^\circ\text{C} \leq T_A \leq +125^\circ\text{C}$		2.5	4	nA
Input Offset Current	I_{OS}	$-40^\circ\text{C} \leq T_A \leq +125^\circ\text{C}$		20	70	pA
AD8571/AD8574		$-40^\circ\text{C} \leq T_A \leq +125^\circ\text{C}$		150	200	pA
AD8572		$-40^\circ\text{C} \leq T_A \leq +85^\circ\text{C}$		30	150	pA
		$-40^\circ\text{C} \leq T_A \leq +125^\circ\text{C}$		150	400	pA
Input Voltage Range			0		5	V
Common-Mode Rejection Ratio	CMRR	$V_{CM} = 0\text{ V to } 5\text{ V}$	120	140		dB
		$-40^\circ\text{C} \leq T_A \leq +125^\circ\text{C}$	115	130		dB
Large Signal Voltage Gain ¹	A_{VO}	$R_L = 10\text{ k}\Omega$, $V_O = 0.3\text{ V to } 4.7\text{ V}$	125	145		dB
		$-40^\circ\text{C} \leq T_A \leq +125^\circ\text{C}$	120	135		dB
Offset Voltage Drift	$\Delta V_{OS}/\Delta T$	$-40^\circ\text{C} \leq T_A \leq +125^\circ\text{C}$		0.005	0.04	$\mu\text{V}/^\circ\text{C}$
OUTPUT CHARACTERISTICS						
Output Voltage High	V_{OH}	$R_L = 100\text{ k}\Omega$ to GND	4.99	4.998		V
		$R_L = 100\text{ k}\Omega$ to GND @ -40°C to $+125^\circ\text{C}$	4.99	4.997		V
		$R_L = 10\text{ k}\Omega$ to GND	4.95	4.98		V
		$R_L = 10\text{ k}\Omega$ to GND @ -40°C to $+125^\circ\text{C}$	4.95	4.975		V
Output Voltage Low	V_{OL}	$R_L = 100\text{ k}\Omega$ to V+		1	10	mV
		$R_L = 100\text{ k}\Omega$ to V+ @ -40°C to $+125^\circ\text{C}$		2	10	mV
		$R_L = 10\text{ k}\Omega$ to V+		10	30	mV
		$R_L = 10\text{ k}\Omega$ to V+ @ -40°C to $+125^\circ\text{C}$		15	30	mV
Short-Circuit Limit	I_{SC}		± 25	± 50		mA
		-40°C to $+125^\circ\text{C}$		± 40		mA
Output Current	I_O			± 30		mA
		-40°C to $+125^\circ\text{C}$		± 15		mA
POWER SUPPLY						
Power Supply Rejection Ratio	PSRR	$V_S = 2.7\text{ V to } 5.5\text{ V}$	120	130		dB
		$-40^\circ\text{C} \leq T_A \leq +125^\circ\text{C}$	115	130		dB
Supply Current per Amplifier	I_{SY}	$V_O = 0\text{ V}$		850	975	μA
		$-40^\circ\text{C} \leq T_A \leq +125^\circ\text{C}$		1000	1075	μA
DYNAMIC PERFORMANCE						
Slew Rate	SR	$R_L = 10\text{ k}\Omega$		0.4		V/ μs
Overload Recovery Time				0.05	0.3	ms
Gain Bandwidth Product	GBP			1.5		MHz
NOISE PERFORMANCE						
Voltage Noise	e_n p-p	0 Hz to 10 Hz		1.3		$\mu\text{V p-p}$
		0 Hz to 1 Hz		0.41		$\mu\text{V p-p}$
Voltage Noise Density	e_n	$f = 1\text{ kHz}$		51		nV/ $\sqrt{\text{Hz}}$
Current Noise Density	i_n	$f = 10\text{ Hz}$		2		fA/ $\sqrt{\text{Hz}}$

¹ Gain testing is dependent upon test bandwidth.

2.7 V ELECTRICAL CHARACTERISTICS

$V_S = 2.7\text{ V}$, $V_{CM} = 1.35\text{ V}$, $V_O = 1.35\text{ V}$, $T_A = 25^\circ\text{C}$, unless otherwise noted.

Table 2.

Parameter	Symbol	Conditions	Min	Typ	Max	Unit
INPUT CHARACTERISTICS						
Offset Voltage	V_{OS}	$-40^\circ\text{C} \leq T_A \leq +125^\circ\text{C}$		1	5	μV
					10	μV
Input Bias Current	I_B	$-40^\circ\text{C} \leq T_A \leq +125^\circ\text{C}$		10	50	pA
AD8571/AD8574		$-40^\circ\text{C} \leq T_A \leq +125^\circ\text{C}$		1.0	1.5	nA
AD8572		$-40^\circ\text{C} \leq T_A \leq +85^\circ\text{C}$		160	300	pA
		$-40^\circ\text{C} \leq T_A \leq +125^\circ\text{C}$		2.5	4	nA
Input Offset Current	I_{OS}	$-40^\circ\text{C} \leq T_A \leq +125^\circ\text{C}$		10	50	pA
AD8571/AD8574		$-40^\circ\text{C} \leq T_A \leq +125^\circ\text{C}$		150	200	pA
AD8572		$-40^\circ\text{C} \leq T_A \leq +85^\circ\text{C}$		30	150	pA
		$-40^\circ\text{C} \leq T_A \leq +125^\circ\text{C}$		150	400	pA
Input Voltage Range			0		2.7	V
Common-Mode Rejection Ratio	CMRR	$V_{CM} = 0\text{ V to } 2.7\text{ V}$	115	130		dB
		$-40^\circ\text{C} \leq T_A \leq +125^\circ\text{C}$	110	130		dB
Large Signal Voltage Gain ¹	A_{VO}	$R_L = 10\text{ k}\Omega$, $V_O = 0.3\text{ V to } 2.4\text{ V}$	110	140		dB
		$-40^\circ\text{C} \leq T_A \leq +125^\circ\text{C}$	105	130		dB
Offset Voltage Drift	$\Delta V_{OS}/\Delta T$	$-40^\circ\text{C} \leq T_A \leq +125^\circ\text{C}$		0.005	0.04	$\mu\text{V}/^\circ\text{C}$
OUTPUT CHARACTERISTICS						
Output Voltage High	V_{OH}	$R_L = 100\text{ k}\Omega$ to GND	2.685	2.697		V
		$R_L = 100\text{ k}\Omega$ to GND @ -40°C to $+125^\circ\text{C}$	2.685	2.696		V
		$R_L = 10\text{ k}\Omega$ to GND	2.67	2.68		V
		$R_L = 10\text{ k}\Omega$ to GND @ -40°C to $+125^\circ\text{C}$	2.67	2.675		V
Output Voltage Low	V_{OL}	$R_L = 100\text{ k}\Omega$ to V_+		1	10	mV
		$R_L = 100\text{ k}\Omega$ to V_+ @ -40°C to $+125^\circ\text{C}$		2	10	mV
		$R_L = 10\text{ k}\Omega$ to V_+		10	20	mV
		$R_L = 10\text{ k}\Omega$ to V_+ @ -40°C to $+125^\circ\text{C}$		15	20	mV
Short-Circuit Limit	I_{SC}		± 10	± 15		mA
		-40°C to $+125^\circ\text{C}$		± 10		mA
Output Current	I_O			± 10		mA
		-40°C to $+125^\circ\text{C}$		± 5		mA
POWER SUPPLY						
Power Supply Rejection Ratio	PSRR	$V_S = 2.7\text{ V to } 5.5\text{ V}$	120	130		dB
		$-40^\circ\text{C} \leq T_A \leq +125^\circ\text{C}$	115	130		dB
Supply Current per Amplifier	I_{SY}	$V_O = 0\text{ V}$		750	900	μA
		$-40^\circ\text{C} \leq T_A \leq +125^\circ\text{C}$		950	1000	μA
DYNAMIC PERFORMANCE						
Slew Rate	SR	$R_L = 10\text{ k}\Omega$		0.5		V/ μs
Overload Recovery Time				0.05		ms
Gain Bandwidth Product	GBP			1		MHz
NOISE PERFORMANCE						
Voltage Noise	e_n p-p	0 Hz to 10 Hz		2.0		$\mu\text{V p-p}$
Voltage Noise Density	e_n	$f = 1\text{ kHz}$		94		nV/ $\sqrt{\text{Hz}}$
Current Noise Density	i_n	$f = 10\text{ Hz}$		2		fA/ $\sqrt{\text{Hz}}$

¹ Gain testing is dependent upon test bandwidth.

ABSOLUTE MAXIMUM RATINGS

Table 3.

Parameter	Rating
Supply Voltage	6 V
Input Voltage	GND – 0.3 V to $V_S + 0.3$ V
Differential Input Voltage ¹	± 5.0 V
ESD (Human Body Model)	2000 V
Output Short-Circuit Duration to GND	Indefinite
Storage Temperature Range	–65°C to +150°C
Operating Temperature Range	–40°C to +125°C
Junction Temperature Range	–65°C to +150°C
Lead Temperature (Soldering, 60 sec)	300°C

¹ Differential input voltage is limited to ± 5.0 V or the supply voltage, whichever is less.

Stresses at or above those listed under Absolute Maximum Ratings may cause permanent damage to the product. This is a stress rating only; functional operation of the product at these or any other conditions above those indicated in the operational section of this specification is not implied. Operation beyond the maximum operating conditions for extended periods may affect product reliability.

THERMAL CHARACTERISTICS

θ_{JA} is specified for the worst-case conditions, that is, θ_{JA} is specified for a device soldered in a circuit board for SOIC and TSSOP packages.

Table 4. Thermal Resistance

Package Type	θ_{JA}	θ_{JC}	Unit
8-Lead SOIC (R)	158	43	°C/W
8-Lead MSOP (RM)	190	44	°C/W
8-Lead TSSOP (RU)	240	43	°C/W
14-Lead SOIC (R)	120	36	°C/W
14-Lead TSSOP (RU)	180	36	°C/W

ESD CAUTION



ESD (electrostatic discharge) sensitive device. Charged devices and circuit boards can discharge without detection. Although this product features patented or proprietary protection circuitry, damage may occur on devices subjected to high energy ESD. Therefore, proper ESD precautions should be taken to avoid performance degradation or loss of functionality.

TYPICAL PERFORMANCE CHARACTERISTICS

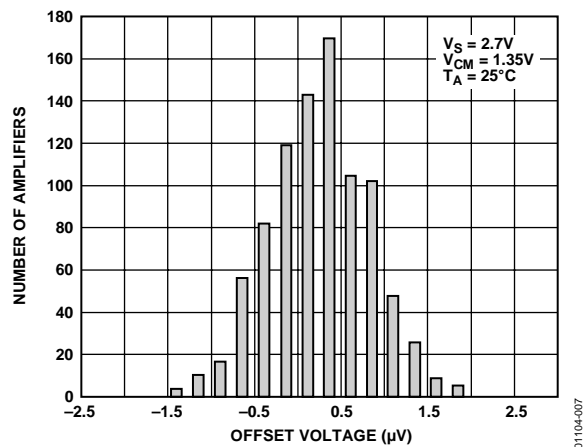


Figure 7. Input Offset Voltage Distribution

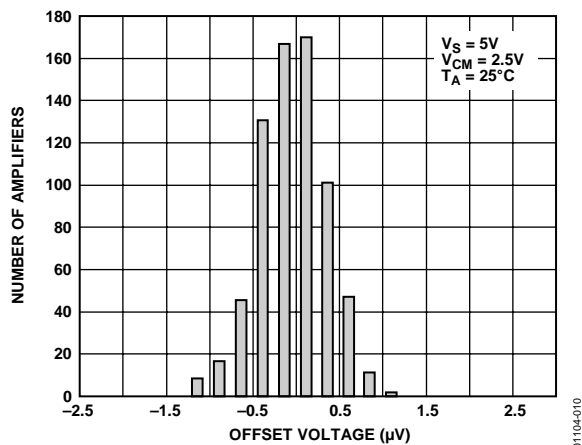


Figure 10. Input Offset Voltage Distribution

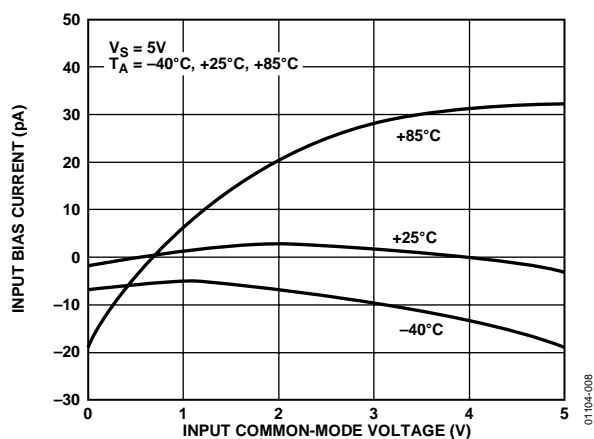


Figure 8. Input Bias Current vs. Input Common-Mode Voltage

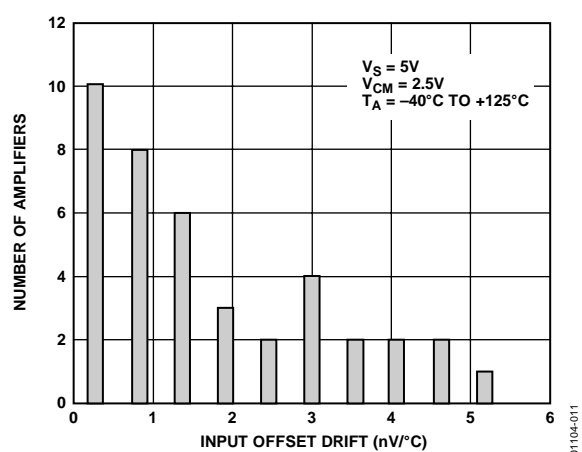


Figure 11. Input Offset Voltage Drift Distribution

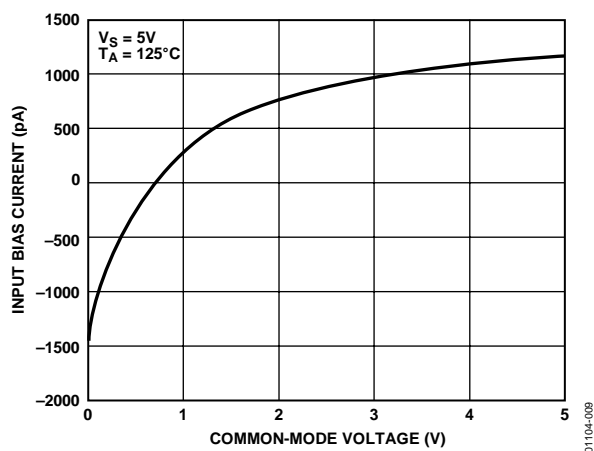


Figure 9. Input Bias Current vs. Common-Mode Voltage

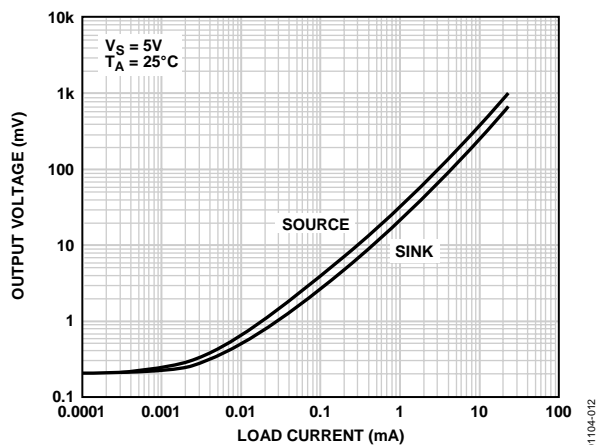


Figure 12. Output Voltage to Supply Rail vs. Load Current

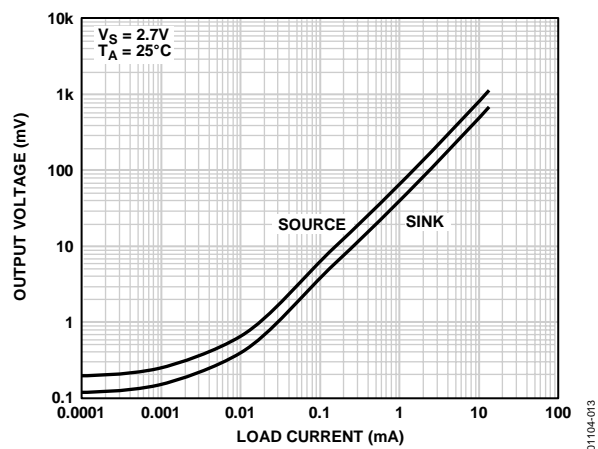


Figure 13. Output Voltage to Supply Rail vs. Load Current

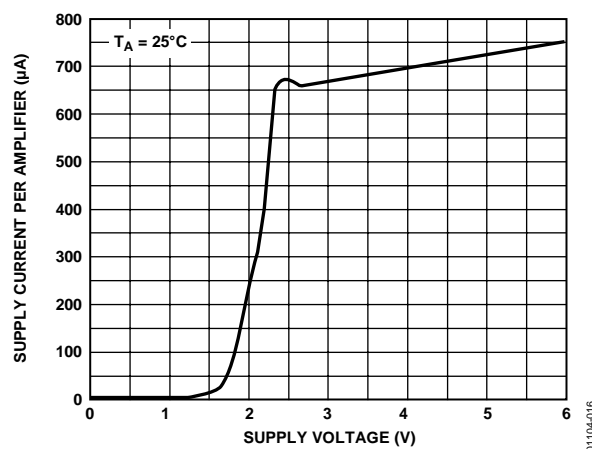


Figure 16. Supply Current per Amplifier vs. Supply Voltage

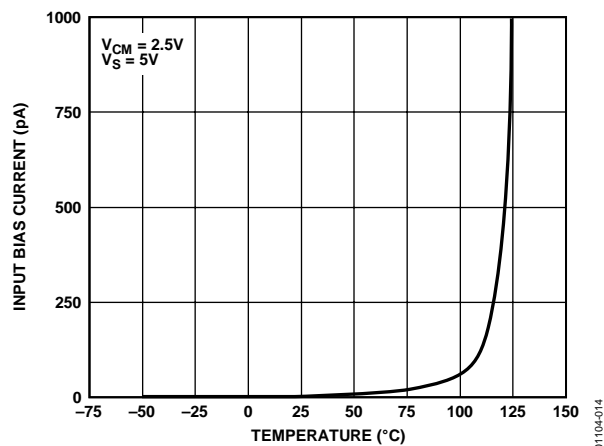


Figure 14. Input Bias Current vs. Temperature

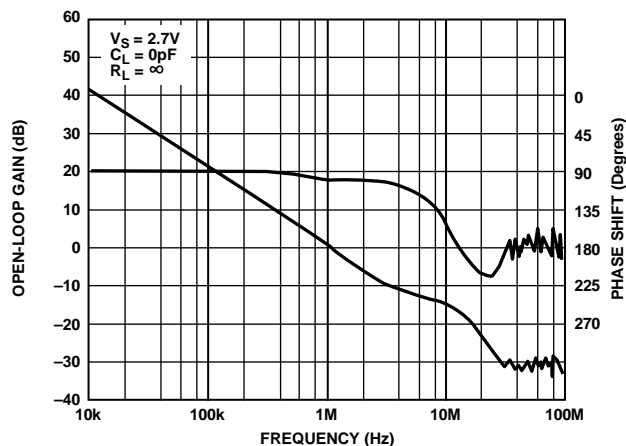


Figure 17. Open-Loop Gain and Phase Shift vs. Frequency

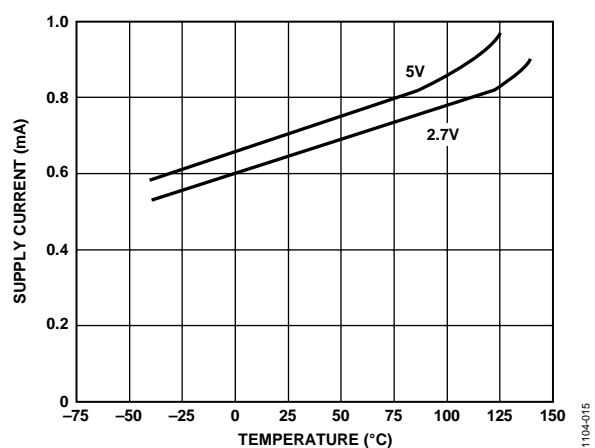


Figure 15. Supply Current vs. Temperature

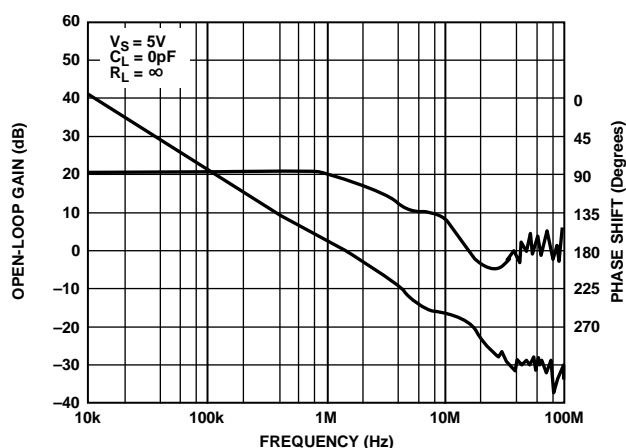


Figure 18. Open-Loop Gain and Phase Shift vs. Frequency

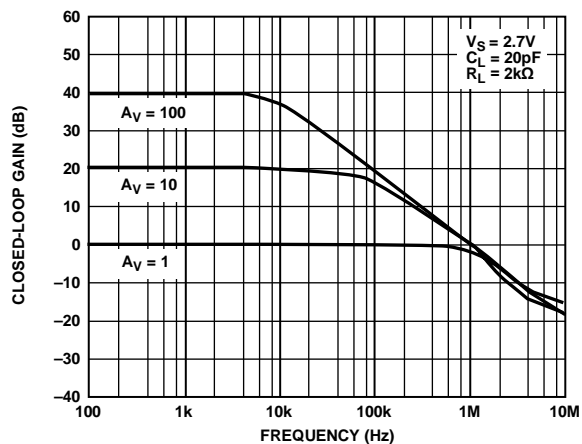


Figure 19. Closed-Loop Gain vs. Frequency

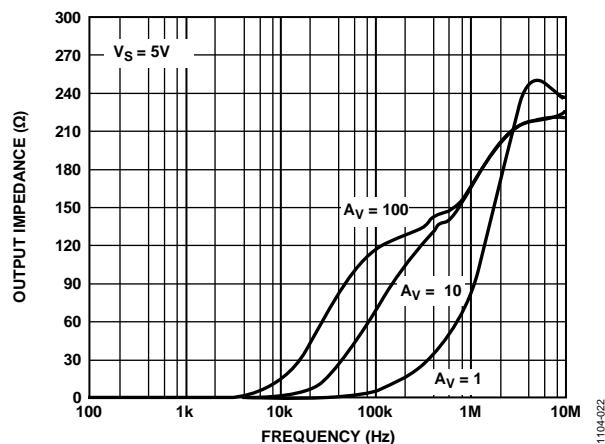


Figure 22. Output Impedance vs. Frequency

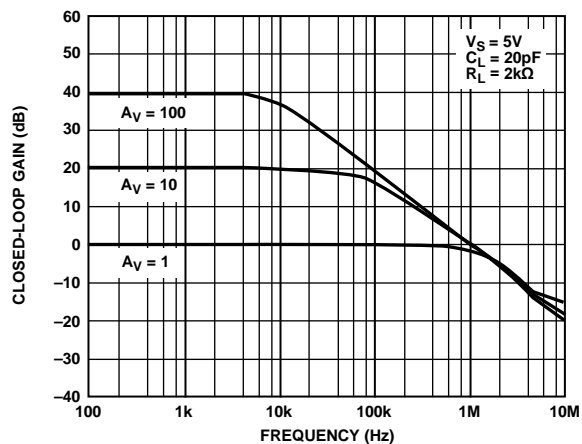


Figure 20. Closed-Loop Gain vs. Frequency

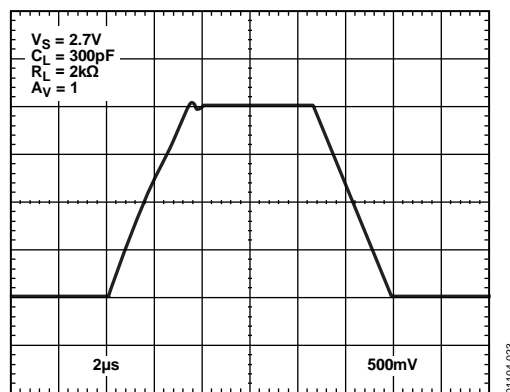


Figure 23. Large Signal Transient Response

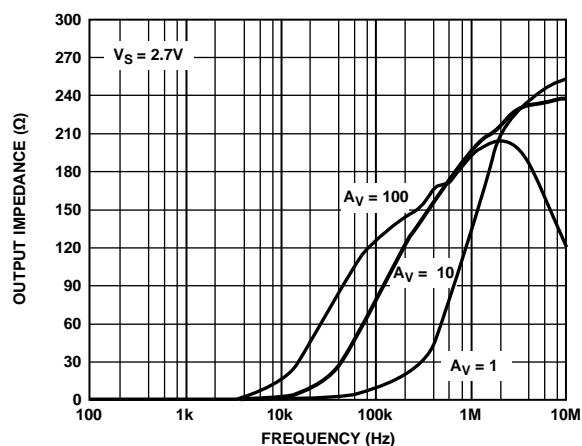


Figure 21. Output Impedance vs. Frequency

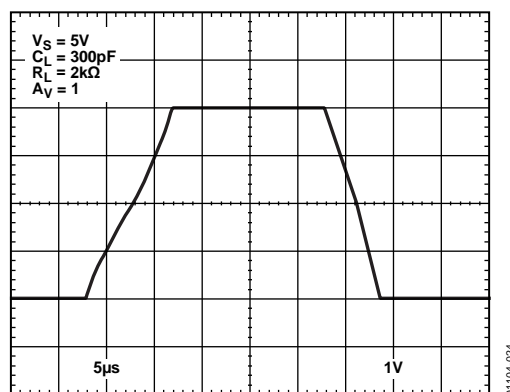


Figure 24. Large Signal Transient Response

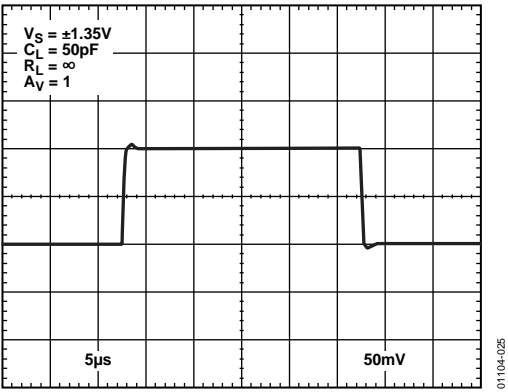


Figure 25. Small Signal Transient Response

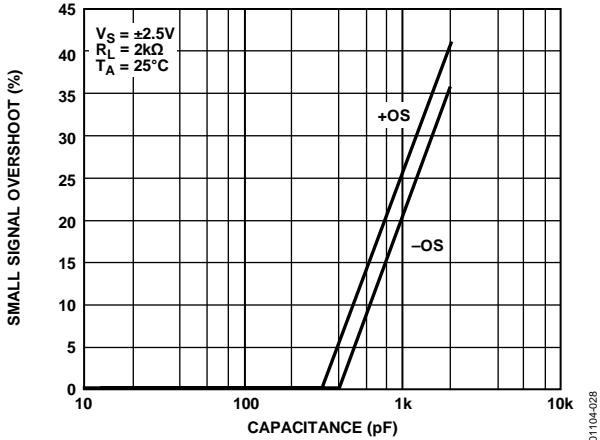


Figure 28. Small Signal Overshoot vs. Load Capacitance

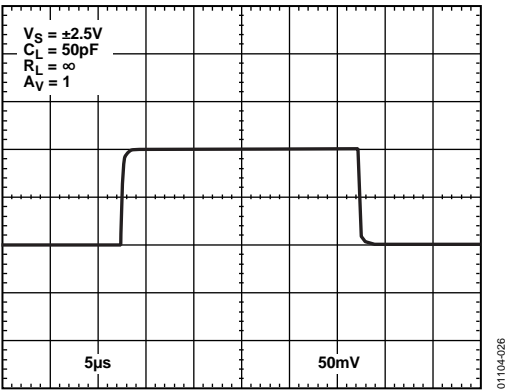


Figure 26. Small Signal Transient Response

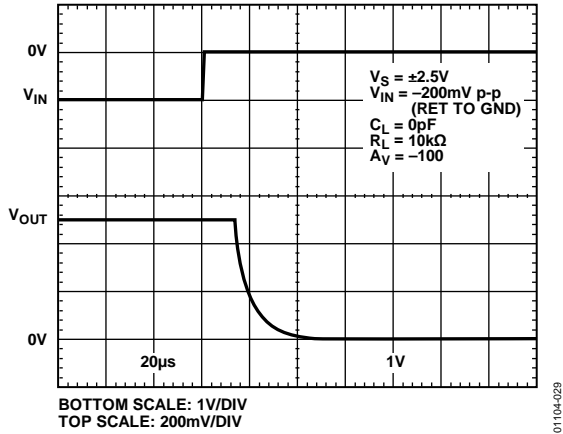


Figure 29. Positive Overvoltage Recovery

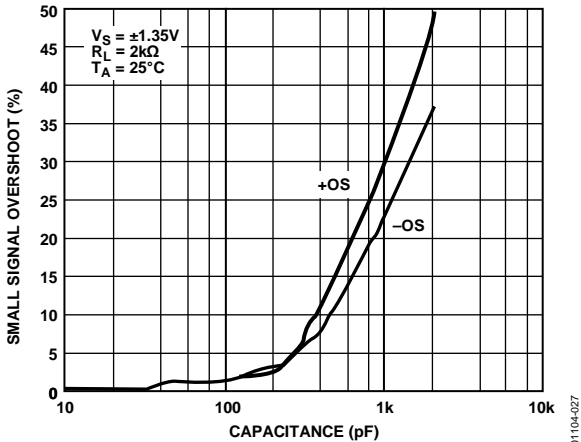


Figure 27. Small Signal Overshoot vs. Load Capacitance

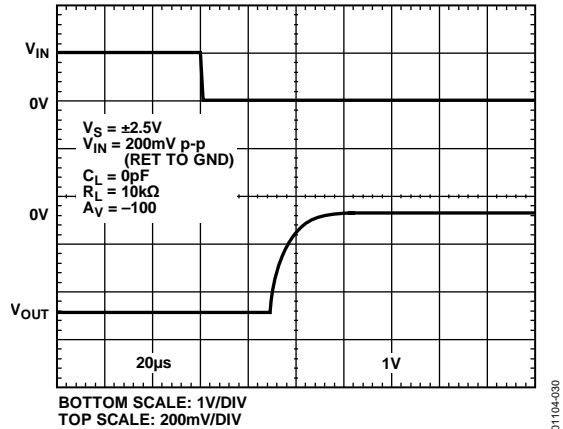


Figure 30. Negative Overvoltage Recovery

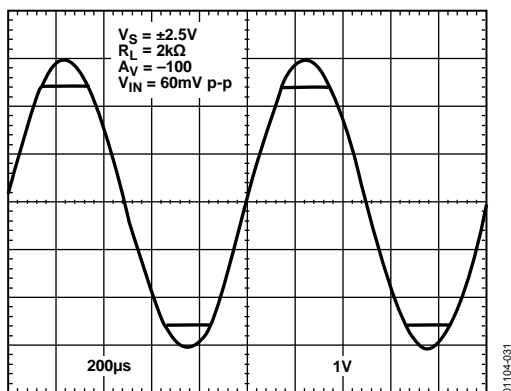


Figure 31. No Phase Reversal

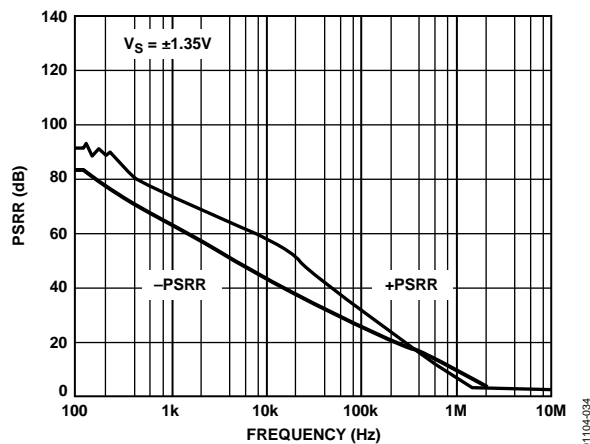


Figure 34. PSRR vs. Frequency

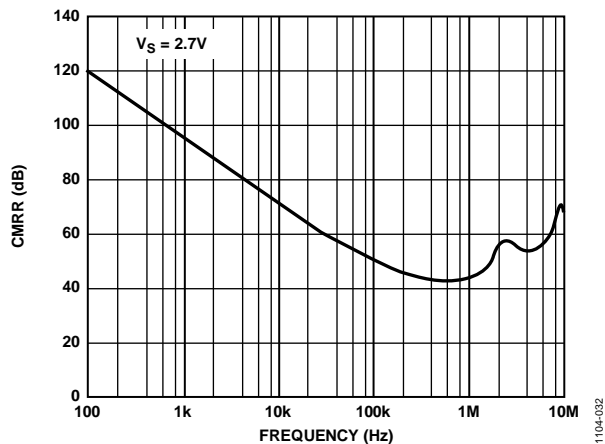


Figure 32. CMRR vs. Frequency

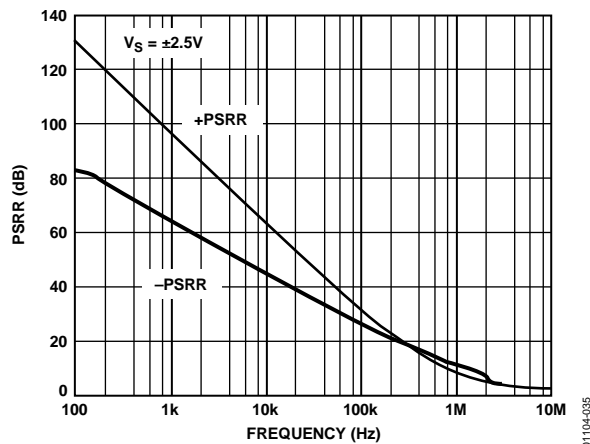


Figure 35. PSRR vs. Frequency

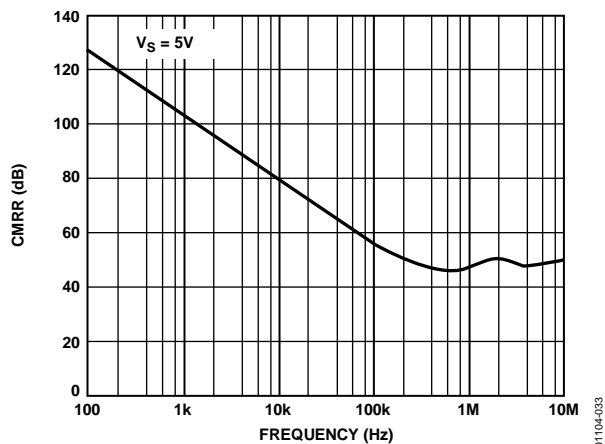


Figure 33. CMRR vs. Frequency

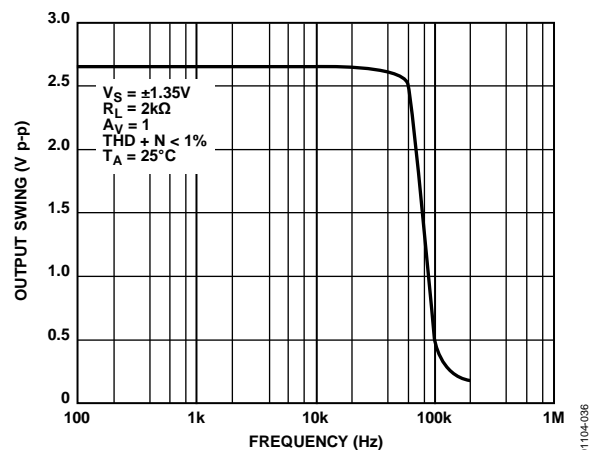


Figure 36. Maximum Output Swing vs. Frequency

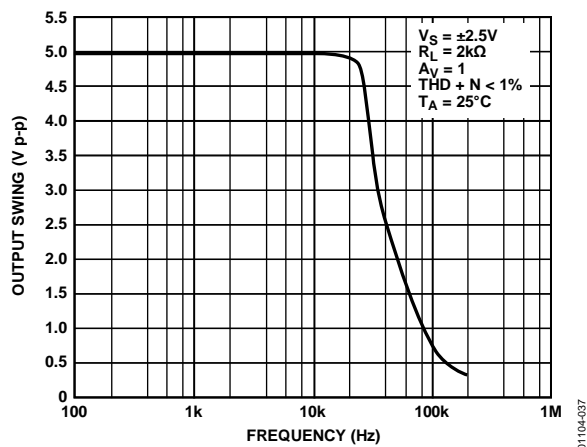


Figure 37. Maximum Output Swing vs. Frequency

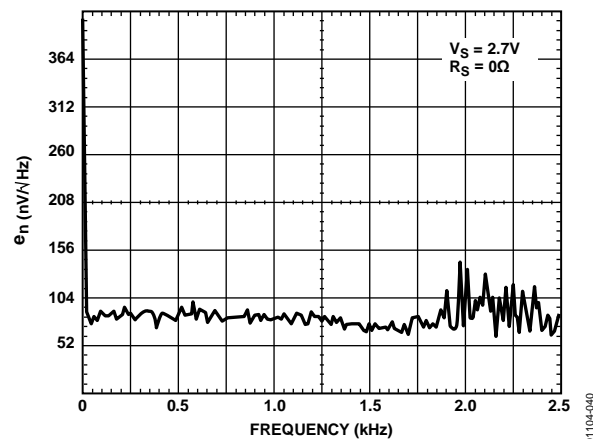


Figure 40. Voltage Noise Density from 0 Hz to 2.5 kHz

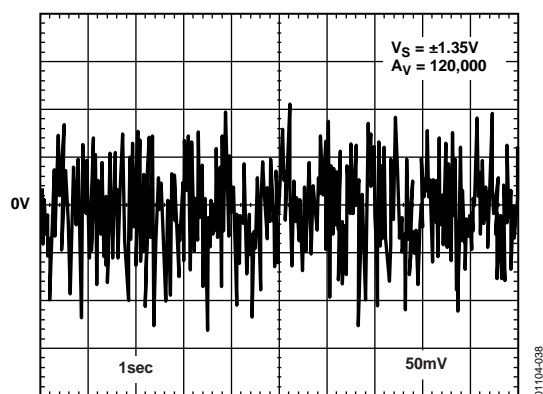


Figure 38. 0.1 Hz to 10 Hz Noise

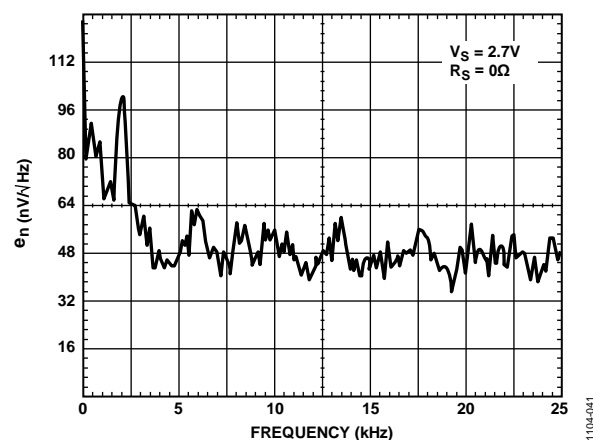


Figure 41. Voltage Noise Density from 0 Hz to 25 kHz

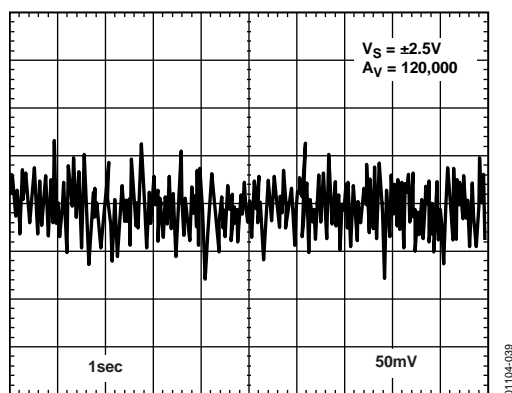


Figure 39. 0.1 Hz to 10 Hz Noise

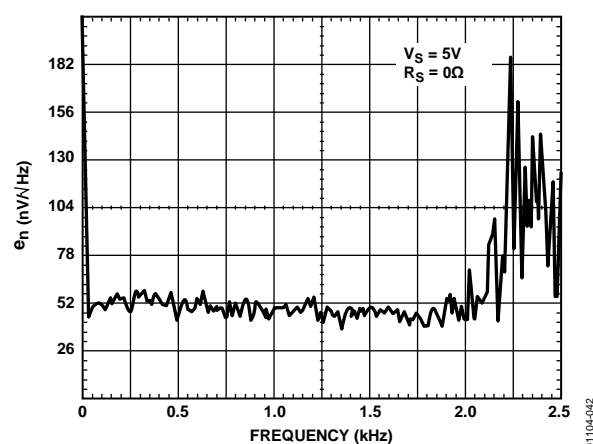


Figure 42. Voltage Noise Density from 0 Hz to 2.5 kHz

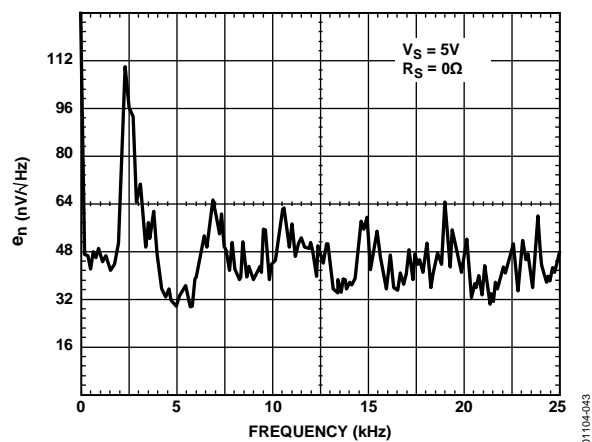


Figure 43. Voltage Noise Density from 0 Hz to 25 kHz

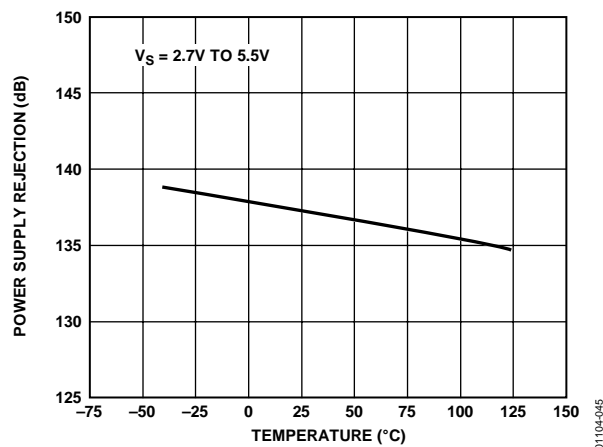


Figure 45. Power Supply Rejection vs. Temperature

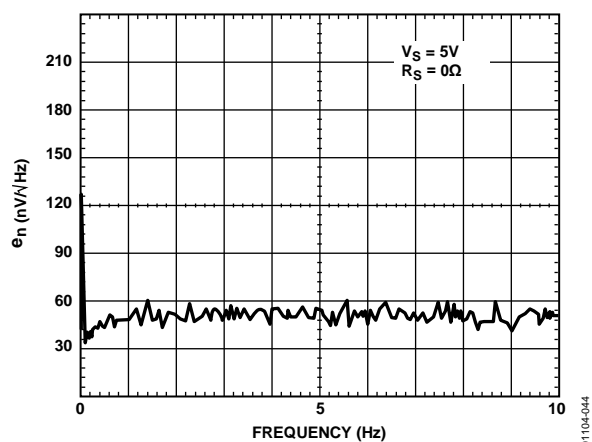


Figure 44. Voltage Noise Density from 0 Hz to 10 Hz

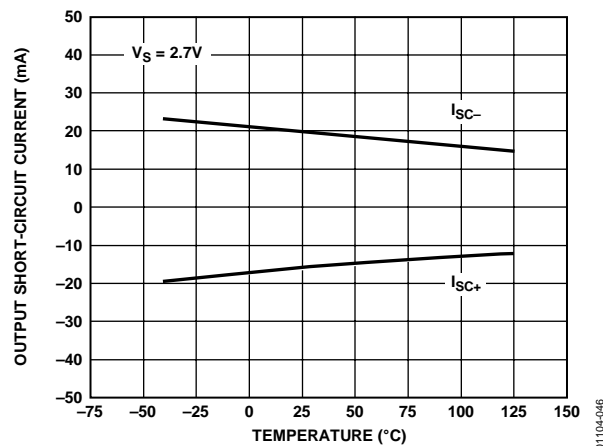


Figure 46. Output Short-Circuit Current vs. Temperature

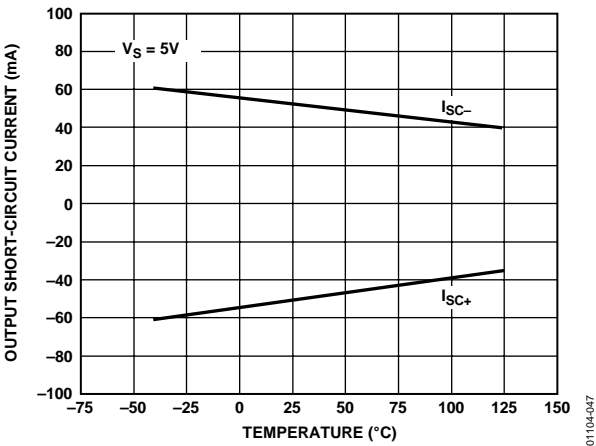


Figure 47. Output Short-Circuit Current vs. Temperature

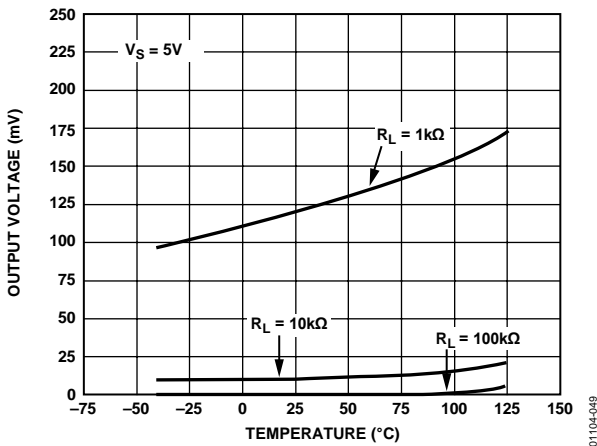


Figure 49. Output Voltage to Supply Rail vs. Temperature

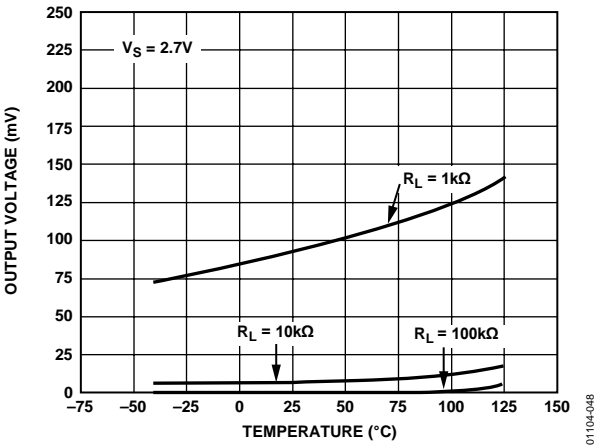


Figure 48. Output Voltage to Supply Rail vs. Temperature

FUNCTIONAL DESCRIPTION

The AD8571/AD8572/AD8574 are CMOS amplifiers that achieve their high degree of precision through random frequency auto-zero stabilization. The autocorrection topology allows the AD8571/AD8572/AD8574 to maintain its low offset voltage over a wide temperature range, and the randomized auto-zero clock eliminates any inter-modulation distortion (IMD) errors at the amplifier output.

The AD8571/AD8572/AD8574 can run from a single-supply voltage as low as 2.7 V. The extremely low offset voltage of 1 μV and no IMD products allow the amplifier to be easily configured for high gains without risk of excessive output voltage errors, which makes the AD8571/AD8572/AD8574 an ideal amplifier for applications requiring both dc precision and low distortion for ac signals. The extremely small temperature drift of 5 nV/ $^{\circ}\text{C}$ ensures a minimum of offset voltage error over its -40°C to $+125^{\circ}\text{C}$ temperature range. These combined features make the AD8571/AD8572/AD8574 an excellent choice for a variety of sensitive measurement and automotive applications.

AMPLIFIER ARCHITECTURE

Each AD8571/AD8572/AD8574 op amp consists of two amplifiers: a main amplifier and a secondary amplifier that is used to correct the offset voltage of the main amplifier. Both consist of a rail-to-rail input stage, allowing the input common-mode voltage range to reach both supply rails. The input stage consists of an NMOS differential pair operating concurrently with a parallel PMOS differential pair. The outputs from the differential input stages are combined in another gain stage whose output is used to drive a rail-to-rail output stage.

The wide voltage swing of the amplifier is achieved by using two output transistors in a common-source configuration. The output voltage range is limited by the drain-to-source resistance of these transistors. As the amplifier is required to source or sink more output current, the voltage drop across these transistors increases due to their on resistance (R_{DS}). Simply put, the output voltage does not swing as close to the rail under heavy output current conditions as it does with light output current. This is a characteristic of all rail-to-rail output amplifiers. Figure 12 and Figure 13 show how close the output voltage can get to the rails with a given output current. The output of the AD8571/AD8572/AD8574 is short-circuit protected to approximately 50 mA of current.

The AD8571/AD8572/AD8574 amplifiers have exceptional gain, yielding greater than 120 dB of open-loop gain with a load of 2 k Ω . Because the output transistors are configured in a common-source configuration, the gain of the output stage, and thus the open-loop gain of the amplifier, is dependent on the load resistance. Open-loop gain decreases with smaller load resistances, which is another characteristic of rail-to-rail output amplifiers.

BASIC AUTO-ZERO AMPLIFIER THEORY

Autocorrection amplifiers are not a new technology. Various IC implementations have been available for more than 15 years, and some improvements have been made over time. The AD8571/AD8572/AD8574 design offers a number of significant performance improvements over older versions while attaining a very substantial reduction in device cost. This section offers a simplified explanation of how the AD8571/AD8572/AD8574 are able to offer extremely low offset voltages and high open-loop gains.

As noted in the Amplifier Architecture section, each AD8571/AD8572/AD8574 op amp contains two internal amplifiers. One is used as the primary amplifier, and the other as an autocorrection, or nulling, amplifier. Each amplifier has an associated input offset voltage that can be modeled as a dc voltage source in series with the noninverting input. In Figure 50 and Figure 51, these are labeled as V_{OSA} and V_{OSB} , where A denotes the nulling amplifier and B denotes the primary amplifier. The open-loop gain for the +IN and -IN inputs of each amplifier is given as A_X . Both amplifiers also have a third voltage input with an associated open-loop gain of B_X .

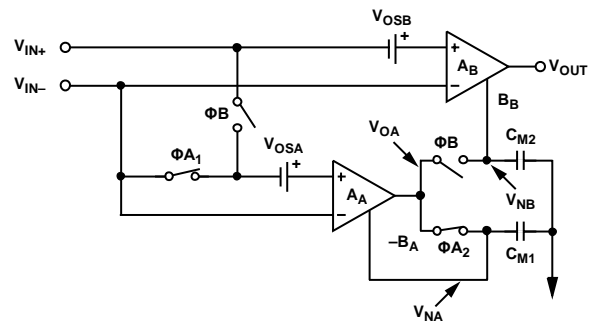


Figure 50. Auto-Zero Phase of the Amplifier

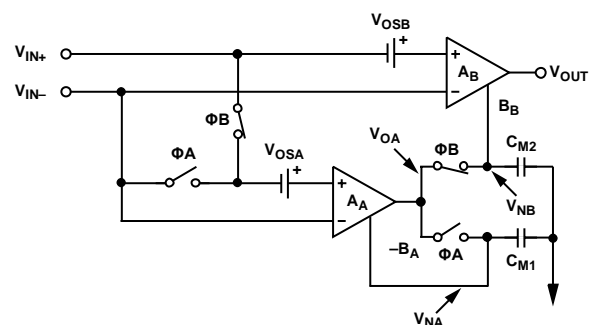


Figure 51. Output Phase of the Amplifier

There are two modes of operation determined by the action of two sets of switches in the amplifier: an auto-zero phase and an amplification phase.

AUTO-ZERO PHASE

In this phase, all Φ_{AX} switches are closed, and all Φ_B switches are open. Here, the nulling amplifier is taken out of the gain loop by shorting its two inputs together. Of course, there is a degree of offset voltage, shown as V_{OSA} , inherent in the nulling amplifier, that maintains a potential difference between the +IN and -IN inputs. The nulling amplifier feedback loop is closed through Φ_{A2} , and V_{OSA} appears at the output of the nulling amplifier and on C_{M1} , an internal capacitor in the AD8571/AD8572/AD8574. Mathematically, this can be expressed in the time domain as

$$V_{OA}[t] = A_A V_{OSA}[t] - B_A V_{OA}[t] \quad (1)$$

This can also be expressed as

$$V_{OA}[t] = \frac{A_A V_{OSA}[t]}{1 + B_A} \quad (2)$$

The previous equations show that the offset voltage of the nulling amplifier times a gain factor appears at the output of the nulling amplifier and thus on the C_{M1} capacitor.

AMPLIFICATION PHASE

When the Φ_B switches close and the Φ_{AX} switches open for the amplification phase, the offset voltage remains on C_{M1} and essentially corrects any error from the nulling amplifier. The voltage across C_{M1} is designated as V_{NA} . The potential difference between the two inputs to the primary amplifier is designated as V_{IN} , or $V_{IN} = (V_{IN+} - V_{IN-})$. The output of the nulling amplifier can then be expressed as

$$V_{OA}[t] = A_A (V_{IN}[t] - V_{OSA}[t]) - B_A V_{NA}[t] \quad (3)$$

Because Φ_{AX} is now open and there is no place for C_{M1} to discharge, the voltage (V_{NA}) at the present time (t) is equal to the voltage at the output of the nulling amp (V_{OA}) at the time when Φ_{AX} is closed. If the period of the autocorrection switching frequency is designated as T_s , the amplifier switches between phases every $0.5 \times T_s$. Therefore, in the amplification phase

$$V_{NA}[t] = V_{OA} \left[t - \frac{1}{2} T_s \right] \quad (4)$$

and substituting Equation 4 and Equation 2 into Equation 3 yields

$$V_{OA}[t] = A_A V_{IN}[t] + A_A V_{OSA}[t] - \frac{A_A B_A V_{OSA} \left[t - \frac{1}{2} T_s \right]}{1 + B_A} \quad (5)$$

For the sake of simplification, it can be assumed that the auto-correction frequency is much faster than any potential change in V_{OSA} or V_{OSB} . This is a good assumption because changes in offset voltage are a function of temperature variation or long-term wear time, both of which are much slower than the auto-zero clock frequency of the AD8571/AD8572/AD8574, which effectively makes the V_{OS} time invariant, and Equation 5 can be rewritten as

$$V_{OA}[t] = A_A V_{IN}[t] + \frac{A_A (1 + B_A) V_{OSA} - A_A B_A V_{OSA}}{1 + B_A} \quad (6)$$

or

$$V_{OA}[t] = A_A \left(V_{IN}[t] + \frac{V_{OSA}}{1 + B_A} \right) \quad (7)$$

Here, the auto-zeroing becomes apparent. Note that the V_{OS} term is reduced by a factor of $1 + B_A$, which shows how the nulling amplifier has greatly reduced its own offset voltage error even before correcting the primary amplifier. Therefore, the primary amplifier output voltage is the voltage at the output of the AD8571/AD8572/AD8574 amplifier. It is equal to

$$V_{OUT}[t] = A_B (V_{IN}[t] + V_{OSB}) + B_B V_{NB} \quad (8)$$

In the amplification phase, $V_{OA} = V_{NB}$, so this can be rewritten as

$$V_{OUT}[t] = A_B V_{IN}[t] + A_B V_{OSB} + B_B \left[A_A \left(V_{IN}[t] + \frac{V_{OSA}}{1 + B_A} \right) \right] \quad (9)$$

Combining terms yield

$$V_{OUT}[t] = V_{IN}[t] (A_B + A_A B_B) + \frac{A_A B_B V_{OSA}}{1 + B_A} + A_B V_{OSB} \quad (10)$$

The AD8571/AD8572/AD8574 architecture is optimized in such a way that $A_A = A_B$, $B_A = B_B$, and $B_A \gg 1$. In addition, the gain product to $A_A B_B$ is much greater than A_B . Therefore, Equation 10 can be simplified to

$$V_{OUT}[t] = V_{IN}[t] A_A B_A + A_A (V_{OSA} + V_{OSB}) \quad (11)$$

Most obvious is the gain product of both the primary and nulling amplifiers. This $A_A B_A$ term is what gives the AD8571/AD8572/AD8574 extremely high open-loop gain. To understand how V_{OSA} and V_{OSB} relate to the overall effective input offset voltage of the complete amplifier, set up the generic amplifier equation of

$$V_{OUT} = k \times (V_{IN} + V_{OS, EFF}) \quad (12)$$

where:

k is the open-loop gain of an amplifier.

$V_{OS, EFF}$ is its effective offset voltage.

Putting Equation 12 into the form of Equation 11 gives

$$V_{OUT}[t] = V_{IN}[t] A_A B_A + V_{OS, EFF} A_A B_A \quad (13)$$

Therefore,

$$V_{OS, EFF} \approx \frac{V_{OSA} + V_{OSB}}{B_A} \quad (14)$$

Thus, the offset voltages of both the primary and nulling amplifiers are reduced by the gain factor B_A , which takes a typical input offset voltage from several millivolts down to an effective input offset voltage of submicrovolts. This autocorrection scheme makes the AD8571/AD8572/AD8574 amplifiers extremely precise.

HIGH GAIN, CMRR, AND PSRR

Common-mode and power supply rejection are indications of the amount of offset voltage an amplifier has as a result of a change in its input common-mode or power supply voltages. As shown in the Amplification Phase section, the autocorrection architecture of the AD8571/AD8572/AD8574 allows it to effectively minimize offset voltages. The technique also corrects for offset errors caused by common-mode voltage swings and power supply variations, which results in superb CMRR and PSRR figures in excess of 130 dB. Because the autocorrection occurs continuously, these figures can be maintained across the temperature range of the device (-40°C to $+125^{\circ}\text{C}$).

MAXIMIZING PERFORMANCE THROUGH PROPER LAYOUT

To achieve the maximum performance of the extremely high input impedance and low offset voltage of the AD8571/AD8572/AD8574, care should be taken in the circuit board layout. The PCB surface must remain clean and free of moisture to avoid leakage currents between adjacent traces. Surface coating of the circuit board reduces surface moisture and provides a humidity barrier, reducing parasitic resistance on the board. The use of guard rings around the amplifier inputs further reduces leakage currents. Figure 52 shows how the guard ring should be configured, and Figure 53 shows the top view of how a surface-mount layout can be arranged. The guard ring does not need to be a specific width, but it should form a continuous loop around both inputs. By setting the guard ring voltage equal to the voltage at the non-inverting input, parasitic capacitance is minimized as well. For further reduction of leakage currents, components can be mounted to the PCB using Teflon® standoff insulators.

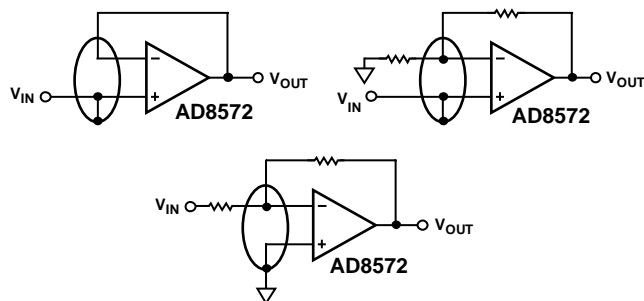


Figure 52. Guard Ring Layout and Connections to Reduce PCB Leakage Currents

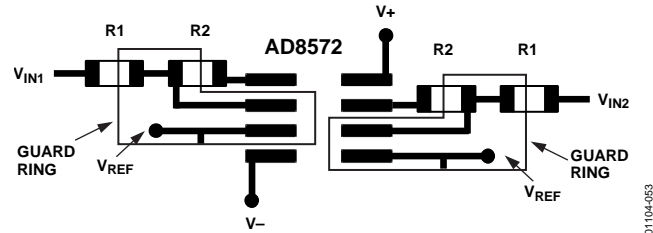


Figure 53. Top View of AD8572 SOIC Layout with Guard Rings

Other potential sources of offset error are thermoelectric voltages on the circuit board. This voltage, also called Seebeck voltage, occurs at the junction of two dissimilar metals and is proportional to the junction temperature. The most common metallic junctions on a circuit board are solder-to-board trace and solder-to-component lead. Figure 54 shows a cross-section view of the thermal voltage error sources. When the temperature of the PCB at one end of the component (T_{A1}) differs from the temperature at the other end (T_{A2}), the Seebeck voltages are not equal, resulting in a thermal voltage error.

This thermocouple error can be reduced by using dummy components to match the thermoelectric error source. Placing the dummy component as close as possible to its partner ensures that both Seebeck voltages are equal, thus canceling the thermocouple error. Maintaining a constant ambient temperature on the circuit board further reduces this error. The use of a ground plane helps distribute heat throughout the board and also reduces EMI noise pickup.

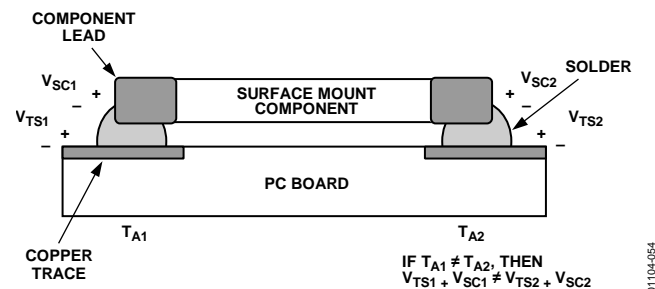
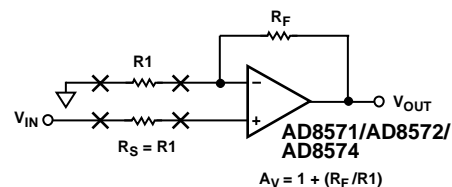


Figure 54. Mismatch in Seebeck Voltages Causes a Thermoelectric Voltage Error



R_S SHOULD BE PLACED IN CLOSE PROXIMITY AND ALIGNMENT TO R_1 TO BALANCE SEEBECK VOLTAGES

Figure 55. Using Dummy Components to Cancel Thermoelectric Voltage Errors

1/f NOISE CHARACTERISTICS

Another advantage of auto-zero amplifiers is their ability to cancel flicker noise. Flicker noise, also known as 1/f noise, is noise inherent in the physics of semiconductor devices and increases 3 dB for every octave decrease in frequency. The 1/f corner frequency of an amplifier is the frequency at which the flicker noise is equal to the broadband noise of the amplifier. At lower frequencies, flicker noise dominates, causing higher degrees of error for sub-Hertz frequencies or dc precision applications.

Because the AD8571/AD8572/AD8574 amplifiers are self-correcting op amps, they do not have increasing flicker noise at lower frequencies. In essence, low frequency noise is treated as a slowly varying offset error and is greatly reduced with autocorrection. The correction becomes more effective as the noise frequency approaches dc, offsetting the tendency of the noise to increase exponentially as frequency decreases, which allows the AD8571/AD8572/AD8574 to have lower noise near dc than standard low noise amplifiers that are susceptible to 1/f noise.

RANDOM AUTO-ZERO CORRECTION ELIMINATES INTERMODULATION DISTORTION

The AD8571/AD8572/AD8574 can be used as conventional op amps for gains up to 1 MHz. The auto-zero correction frequency of the device continuously varies, based on a pseudorandom generator with a uniform distribution from 2 kHz to 4 kHz. The randomization of the autocorrection clock creates a continuous randomization of IMD products that show up as simple broadband noise at the output of the amplifier. This broadband noise naturally combines with the amplifier voltage noise in a root-squared-sum fashion, resulting in an output free of IMD. Figure 56 shows the spectral output of an AD8572 with the amplifier configured for unity gain and the input grounded. Figure 57 shows the spectral output with the amplifier configured for a gain of 60 dB.

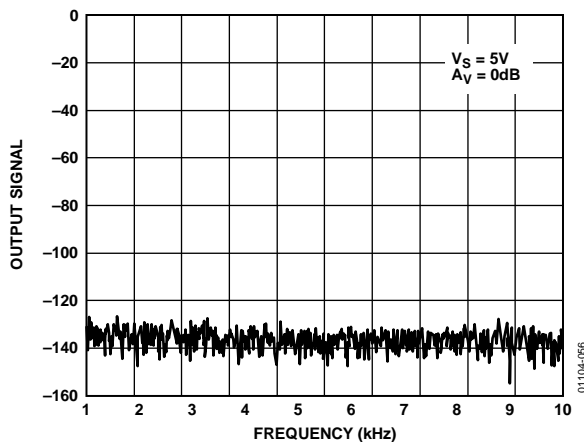


Figure 56. Spectral Analysis of AD8572 Output in Unity Gain Configuration

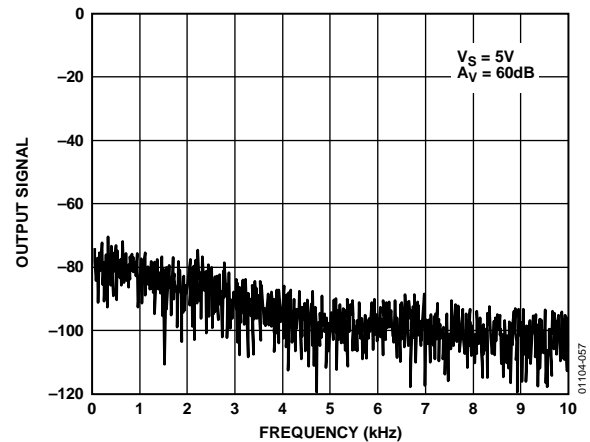


Figure 57. Spectral Analysis of AD8571/AD8572/AD8574 Output with 60 dB Gain

Figure 58 shows the spectral output of an AD8572 configured in a high gain (60 dB) with a 1 mV input signal applied. Note the absence of any IMD products in the spectrum. The signal-to-noise ratio (SNR) of the output signal is better than 60 dB, or 0.1%.

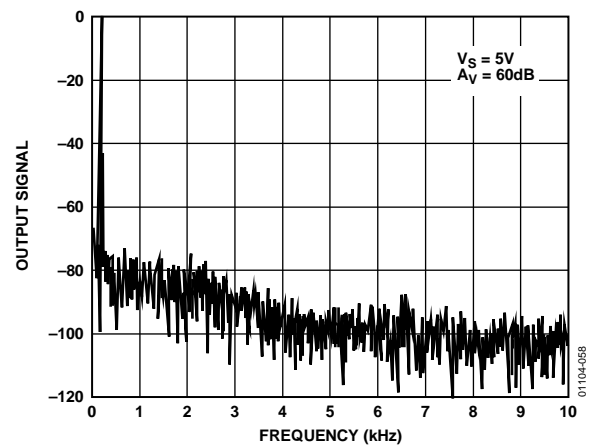


Figure 58. Spectral Analysis of AD8572 in High Gain with an Input Signal

BROADBAND AND EXTERNAL RESISTOR NOISE CONSIDERATIONS

The total broadband noise output from any amplifier is primarily a function of three types of noise: input voltage noise from the amplifier, input current noise from the amplifier, and Johnson noise from the external resistors used around the amplifier. Input voltage noise, or e_n , is strictly a function of the amplifier used. The Johnson noise from a resistor is a function of the resistance and the temperature. Input current noise, or i_n , creates an equivalent voltage noise proportional to the resistors used around the amplifier. These noise sources are not correlated with each other and their combined noise sums in a root-squared-sum fashion. The full equation is given as

$$e_{n, \text{TOTAL}} = [e_n^2 + 4kTr_s + (i_n r_s)^2]^{1/2} \quad (15)$$

where:

e_n is the input voltage noise of the amplifier.

i_n is the input current noise of the amplifier.

r_s is the source resistance connected to the noninverting terminal.

k is Boltzmann's constant (1.38×10^{-23} J/K).

T is the ambient temperature in Kelvin ($K = 273.15 + ^\circ\text{C}$).

The input voltage noise density, e_n , of the AD8571/AD8572/AD8574 is 51 nV/ $\sqrt{\text{Hz}}$, and the input noise, i_n , is 2 fA/ $\sqrt{\text{Hz}}$. The $e_{n, \text{TOTAL}}$ is dominated by the input voltage noise provided that the source resistance is less than 172 k Ω . With source resistance greater than 172 k Ω , the overall noise of the system is dominated by the Johnson noise of the resistor itself.

Because the input current noise of the AD8571/AD8572/AD8574 is very small, i_n does not become a dominant term unless $r_s > 4$ G Ω , which is an impractical value of source resistance.

The total noise, $e_{n, \text{TOTAL}}$, is expressed in volts-per-square-root Hertz, and the equivalent rms noise over a certain bandwidth can be found as

$$e_n = e_{n, \text{TOTAL}} \times \sqrt{BW} \quad (16)$$

where BW is the bandwidth of interest in Hertz.

OUTPUT OVERDRIVE RECOVERY

The AD8571/AD8572/AD8574 amplifiers have an excellent overdrive recovery of only 200 μs from either supply rail. This characteristic is particularly difficult for autocorrection amplifiers because the nulling amplifier requires a substantial amount of time to error correct the main amplifier back to a valid output. Figure 29 and Figure 30 show the positive and negative overdrive recovery times for the AD8571/AD8572/AD8574.

The output overdrive recovery for an autocorrection amplifier is defined as the time it takes for the output to correct to its final voltage from an overload state. It is measured by placing the amplifier in a high gain configuration with an input signal that forces the output voltage to the supply rail. The input voltage is then stepped down to the linear region of the amplifier, usually to halfway between the supplies. The time from the input signal step-down to the output settling to within 100 μV of its final value is the overdrive recovery time. Many autocorrection amplifiers require a number of auto-zero clock cycles to recover from output overdrive, and some can take several milliseconds for the output to settle properly.

INPUT OVERVOLTAGE PROTECTION

Although the AD8571/AD8572/AD8574 are rail-to-rail input amplifiers, care should be taken to ensure that the potential difference between the inputs does not exceed 5 V. Under normal operating conditions, the amplifier corrects its output to ensure that the two inputs are at the same voltage. However, if the device is configured as a comparator, or is under some unusual operating condition, the input voltages may be forced to different potentials, which could cause excessive current to flow through the internal diodes in the AD8571/AD8572/AD8574 used to protect the input stage against overvoltage.

If either input exceeds either supply rail by more than 0.3 V, large amounts of current begin to flow through the ESD protection diodes in the amplifier. These diodes are connected between the inputs and each supply rail to protect the input transistors against an electrostatic discharge event and are normally reverse-biased. However, if the input voltage exceeds the supply voltage, these ESD diodes become forward-biased. Without current-limiting, excessive amounts of current can flow through these diodes, causing permanent damage to the device. If inputs are subject to overvoltage, appropriate series resistors should be inserted to limit the diode current to less than 2 mA.

OUTPUT PHASE REVERSAL

Output phase reversal occurs in some amplifiers when the input common-mode voltage range is exceeded. As common-mode voltage moves outside the common-mode range, the outputs of these amplifiers suddenly jump in the opposite direction to the supply rail. This is the result of the differential input pair shutting down, causing a radical shifting of internal voltages that results in the erratic output behavior.

The AD8571/AD8572/AD8574 amplifiers have been carefully designed to prevent any output phase reversal, provided that both inputs are maintained within the supply voltages. If one or both inputs exceed either supply voltage, a resistor should be placed in series with the input to limit the current to less than 2 mA to ensure that the output does not reverse its phase.

CAPACITIVE LOAD DRIVE

The AD8571/AD8572/AD8574 have excellent capacitive load driving capabilities and can safely drive up to 10 nF from a single 5 V supply. Although the device is stable, capacitive loading limits the bandwidth of the amplifier. Capacitive loads also increase the amount of overshoot and ringing at the output. The RC snubber network shown in Figure 59 can be used to reduce the capacitive load ringing and overshoot.

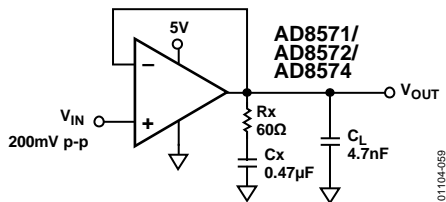


Figure 59. Snubber Network Configuration for Driving Capacitive Loads

Although the snubber network does not recover the loss of amplifier bandwidth from the load capacitance, it does allow the amplifier to drive larger values of capacitance while maintaining a minimum of overshoot and ringing. Figure 60 shows the output of an AD8571/AD8572/AD8574 driving a 1 nF capacitor with and without a snubber network.

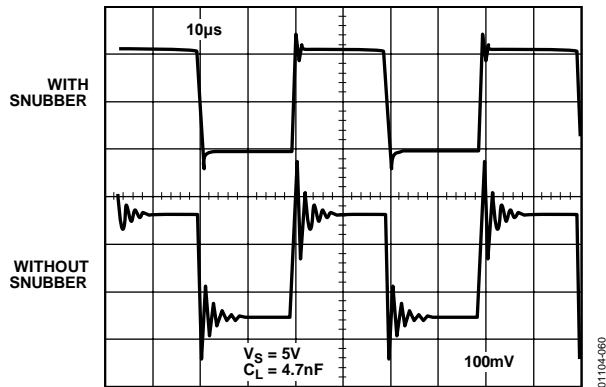


Figure 60. Overshoot and Ringing Are Substantially Reduced Using a Snubber Network

The optimum value for the resistor and capacitor is a function of the load capacitance and is best determined empirically because actual CL includes stray capacitances and can differ substantially from the nominal capacitive load. Table 5 shows some snubber network values that can be used as starting points.

Table 5. Snubber Network Values for Driving Capacitive Loads

CL (nF)	Rx (Ω)	Cx
1	200	1 nF
4.7	60	0.47 μF
10	20	10 μF

POWER-UP BEHAVIOR

At power-up, the AD8571/AD8572/AD8574 settle to a valid output within 5 μs. Figure 61 shows an oscilloscope photo of the output of the amplifier along with the power supply voltage. Figure 62 shows the test circuit. With the amplifier configured for unity gain, the device takes approximately 5 μs to settle to its final output voltage, hundreds of microseconds faster than many other autocorrection amplifiers.

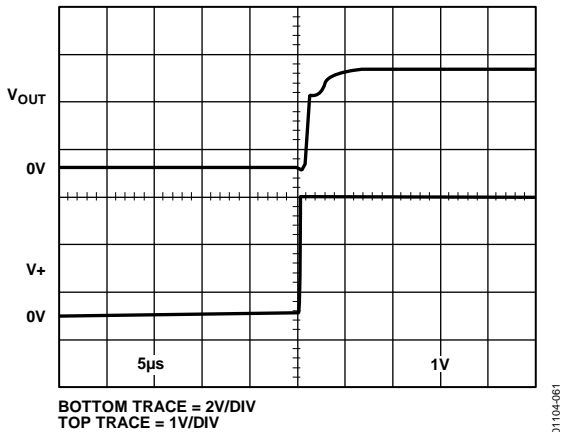


Figure 61. AD8571/AD8572/AD8574 Output Behavior at Power-Up

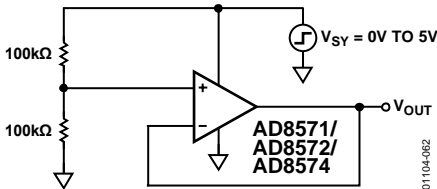


Figure 62. AD8571/AD8572/AD8574 Test Circuit for Power-Up Time

APPLICATIONS INFORMATION

5 V PRECISION STRAIN GAGE CIRCUIT

The extremely low offset voltage of the [AD8572](#) makes it an ideal amplifier for any application requiring accuracy with high gains, such as a weigh scale or strain gage. Figure 63 shows a configuration for a single-supply, precision strain gage measurement system.

The [REF192](#) provides a 2.5 V precision reference voltage for A2. The A2 amplifier boosts this voltage to provide a 4.0 V reference for the top of the strain gage resistor bridge. Q1 provides the current drive for the 350 Ω bridge network. A1 is used to amplify the output of the bridge with the full-scale output voltage equal to

$$\frac{2 \times (R1 + R2)}{R_B} \quad (17)$$

where R_B is the resistance of the load cell.

Using the values given in Figure 63, the output voltage linearly varies from 0 V with no strain to 4 V under full strain.

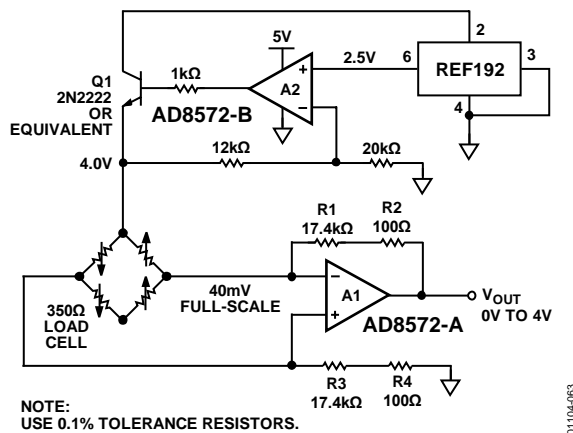


Figure 63. 5 V Precision Strain Gage Amplifier

3 V INSTRUMENTATION AMPLIFIER

The high common-mode rejection, high open-loop gain, and operation down to 3 V of the supply voltage make the [AD8571/AD8572/AD8574](#) an excellent op amp choice for discrete single-supply instrumentation amplifiers. The common-mode rejection ratio of the [AD8571/AD8572/AD8574](#) is greater than 120 dB, but the CMRR of the system is also a function of the external resistor tolerances. The gain of the difference amplifier shown in Figure 64 is given as

$$V_{OUT} = V1 \left(\frac{R4}{R3 + R4} \right) \left(1 + \frac{R1}{R2} \right) - V2 \left(\frac{R2}{R1} \right) \quad (18)$$

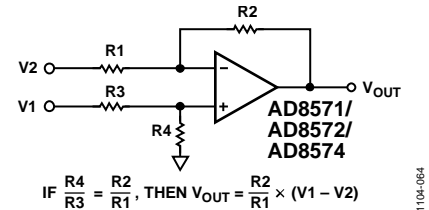


Figure 64. Using the [AD8571/AD8572/AD8574](#) as a Difference Amplifier

In an ideal difference amplifier, the ratio of the resistors is set equal to

$$A_V = \frac{R2}{R1} = \frac{R4}{R3} \quad (19)$$

Set the output voltage of the system to

$$V_{OUT} = A_V (V1 - V2) \quad (20)$$

Due to finite component tolerance, the ratio between the four resistors is not exactly equal, and any mismatch results in a reduction of common-mode rejection from the system. Referring to Figure 64, the exact common-mode rejection ratio can be expressed as

$$CMRR = \frac{R1R4 + 2R2R4 + R2R3}{2R1R4 - 2R2R3} \quad (21)$$

In the 3-op amp instrumentation amplifier configuration shown in Figure 65, the output difference amplifier is set to unity gain with all four resistors equal in value. If the tolerance of the resistors used in the circuit is given as δ , the worst-case CMRR of the instrumentation amplifier is

$$CMRR_{MIN} = \frac{1}{2\delta} \quad (22)$$

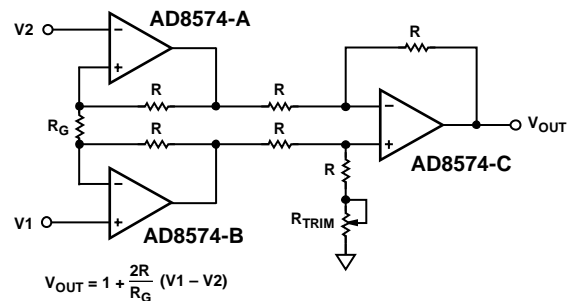


Figure 65. Discrete Instrumentation Amplifier Configuration

Therefore, using 1% tolerance resistors results in a worst-case system CMRR of 0.02, or 34 dB. To achieve high common-mode rejection, either high precision resistors or an additional trimming resistor, as shown in Figure 65, should be used. The value of this trimming resistor should be equal to the value of R multiplied by its tolerance. For example, using 10 k Ω resistors with 1% tolerance would require a series trimming resistor equal to 100 Ω .

HIGH ACCURACY THERMOCOUPLE AMPLIFIER

Figure 66 shows a K-type thermocouple amplifier configuration with cold-junction compensation. Even from a 5 V supply, the AD8571 can provide enough accuracy to achieve a resolution of better than 0.02°C from 0°C to 500°C. D1 is used as a temperature measuring device to correct the cold-junction error from the thermocouple and should be placed as close as possible to the two terminating junctions. With the thermocouple measuring tip immersed in a 0°C ice bath, R6 should be adjusted until the output is at 0 V.

Using the values shown in Figure 66, the output voltage tracks temperature at 10 mV/°C. For a wider range of temperature measurement, R9 can be decreased to 62 kΩ. This creates a 5 mV/°C change at the output, allowing measurements of up to 1000°C.

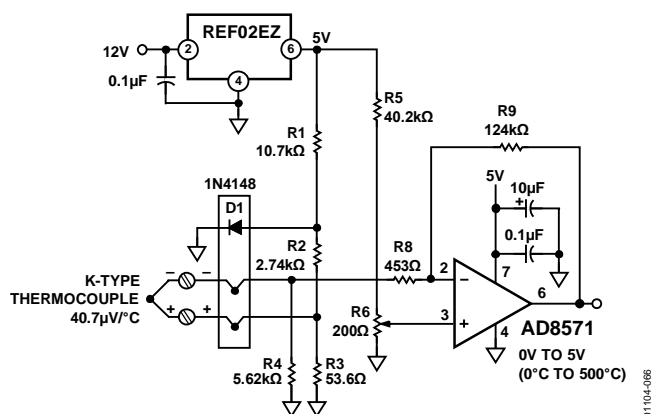


Figure 66. Precision K-Type Thermocouple Amplifier with Cold-Junction Compensation

PRECISION CURRENT METER

Because of its low input bias current and superb offset voltage at single-supply voltages, the AD8571/AD8572/AD8574 are excellent amplifiers for precision current monitoring. Its rail-to-rail input allows the amplifier to be used as either a high-side or a low-side current monitor. Using both amplifiers in the AD8572 provides a simple method to monitor both current supply and return paths for load or fault detection.

Figure 67 shows a high-side current monitor configuration. Here, the input common-mode voltage of the amplifier is at or near the positive supply voltage. The rail-to-rail input of the amplifier provides a precise measurement, even with the input common-mode voltage at the supply voltage. The CMOS input structure does not draw any input bias current, ensuring a minimum of measurement error.

The 0.1 Ω resistor creates a voltage drop to the noninverting input of the AD8571/AD8572/AD8574. The output of the amplifier is corrected until this voltage appears at the inverting input, which creates a current through R1 that in turn flows

through R2. The monitor output is given by

$$\text{Monitor Output} = R2 \times (R_{\text{SENSE}}/R1) \times I_L \quad (23)$$

Using the components shown in Figure 67, the monitor output transfer function is 2.49 V/A.

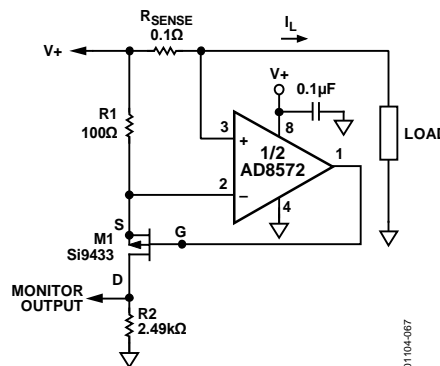


Figure 67. High-Side Load Current Monitor

Figure 68 shows the low-side monitor equivalent. In this circuit, the input common-mode voltage to the AD8572 is at or near ground. Again, a 0.1 Ω resistor provides a voltage drop proportional to the return current. The output voltage is given as

$$\text{Monitor Output} = V_+ - \left(\frac{R2}{R1} \times R_{\text{SENSE}} \times I_L \right) \quad (24)$$

For the component values shown in Figure 68, the monitor output transfer function is $V_+ - 2.49 \text{ V/A}$.

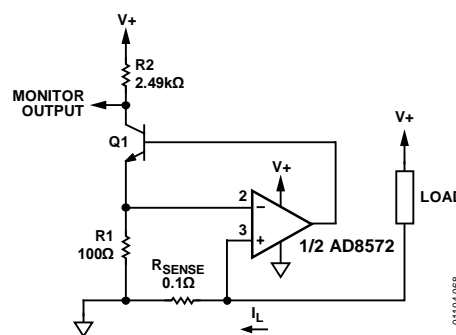


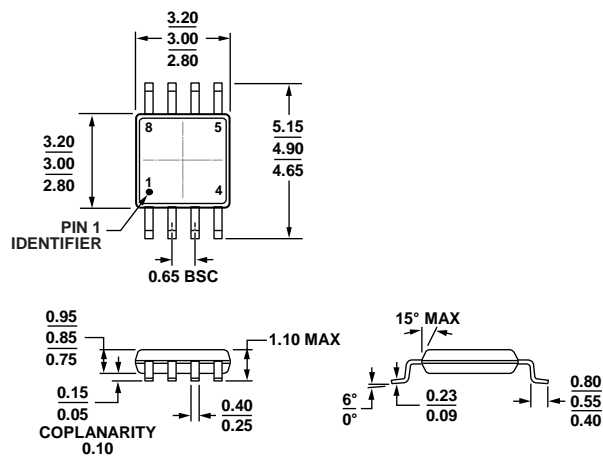
Figure 68. Low-Side Load Current Monitor

PRECISION VOLTAGE COMPARATOR

The AD8571/AD8572/AD8574 can be operated open loop and used as a precision comparator. The AD8571/AD8572/AD8574 have less than 50 µV of offset voltage when they run in this configuration. The slight increase of offset voltage stems from the fact that the autocorrection architecture operates with the lowest offset in a closed-loop configuration, that is, one with negative feedback. With 50 mV of overdrive, the device has a propagation delay of 15 µs on the rising edge and 8 µs on the falling edge.

Care should be taken to ensure that the maximum differential voltage of the device is not exceeded. For more information, see the Input Overvoltage Protection section.

OUTLINE DIMENSIONS

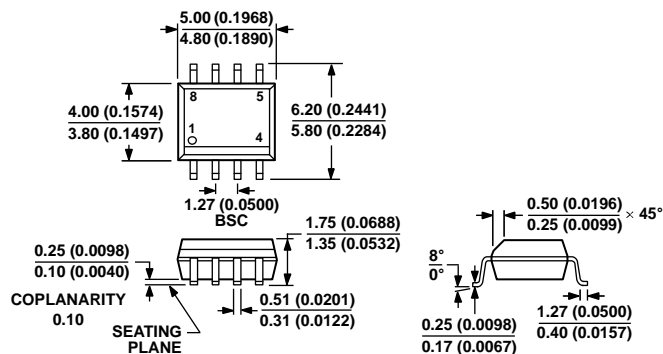


COMPLIANT TO JEDEC STANDARDS MO-187-AA

Figure 69. 8-Lead Mini Small Outline Package [MSOP]
(RM-8)

Dimensions shown in millimeters

10-07-2009-B



COMPLIANT TO JEDEC STANDARDS MS-012-AA

CONTROLLING DIMENSIONS ARE IN MILLIMETERS; INCH DIMENSIONS
(IN PARENTHESES) ARE ROUNDED-OFF MILLIMETER EQUIVALENTS FOR
REFERENCE ONLY AND ARE NOT APPROPRIATE FOR USE IN DESIGN.Figure 70. 8-Lead Standard Small Outline Package [SOIC_N]
Narrow Body (R-8)

Dimensions shown in millimeters and (inches)

012407-A

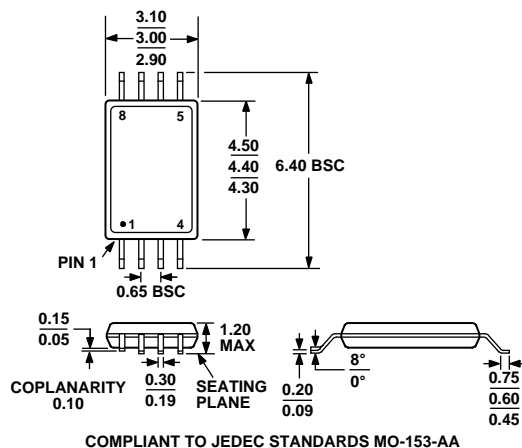


Figure 71. 8-Lead Thin Shrink Small Outline Package [TSSOP]
(RU-8)

Dimensions shown in millimeters

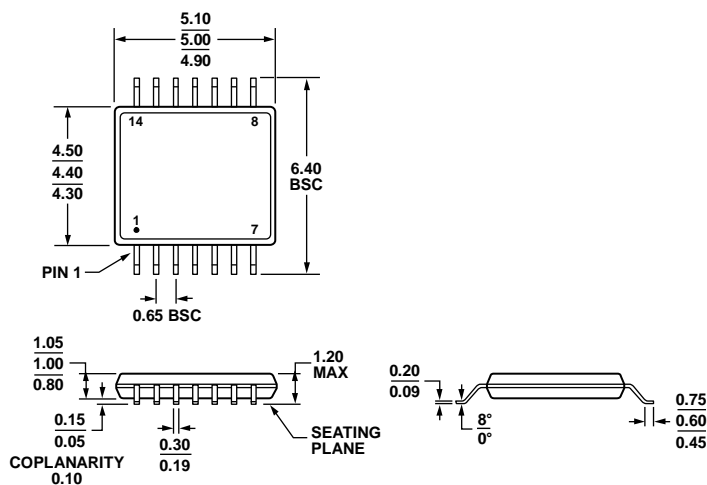
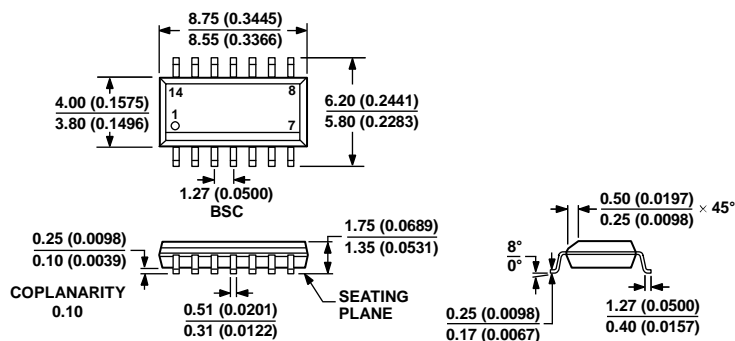


Figure 72. 14-Lead Thin Shrink Small Outline Package [TSSOP]
(RU-14)

Dimensions shown in millimeters

061908-A



COMPLIANT TO JEDEC STANDARDS MS-012-AB
CONTROLLING DIMENSIONS ARE IN MILLIMETERS; INCH DIMENSIONS
(IN PARENTHESES) ARE ROUNDED-OFF MILLIMETER EQUIVALENTS FOR
REFERENCE ONLY AND ARE NOT APPROPRIATE FOR USE IN DESIGN.

Figure 73. 14-Lead Standard Small Outline Package [SOIC_N]
Narrow Body (R-14)
Dimensions shown in millimeters and (inches)

060606-A

ORDERING GUIDE

Model ¹	Temperature Range	Package Description	Package Option	Branding
AD8571ARZ	−40°C to +125°C	8-Lead SOIC_N	R-8	AJA#
AD8571ARZ-REEL	−40°C to +125°C	8-Lead SOIC_N	R-8	
AD8571ARZ-REEL7	−40°C to +125°C	8-Lead SOIC_N	R-8	
AD8571ARMZ	−40°C to +125°C	8-Lead MSOP	RM-8	
AD8571ARMZ-REEL	−40°C to +125°C	8-Lead MSOP	RM-8	
AD8572AR	−40°C to +125°C	8-Lead SOIC_N	R-8	
AD8572AR-REEL	−40°C to +125°C	8-Lead SOIC_N	R-8	
AD8572AR-REEL7	−40°C to +125°C	8-Lead SOIC_N	R-8	
AD8572ARZ	−40°C to +125°C	8-Lead SOIC_N	R-8	
AD8572ARZ-REEL	−40°C to +125°C	8-Lead SOIC_N	R-8	
AD8572ARZ-REEL7	−40°C to +125°C	8-Lead SOIC_N	R-8	
AD8572ARUZ	−40°C to +125°C	8-Lead TSSOP	RU-8	
AD8572ARUZ-REEL	−40°C to +125°C	8-Lead TSSOP	RU-8	
AD8574ARZ	−40°C to +125°C	14-Lead SOIC_N	R-14	
AD8574ARZ-REEL	−40°C to +125°C	14-Lead SOIC_N	R-14	
AD8574ARZ-REEL7	−40°C to +125°C	14-Lead SOIC_N	R-14	
AD8574ARU	−40°C to +125°C	14-Lead TSSOP	RU-14	
AD8574ARU-REEL	−40°C to +125°C	14-Lead TSSOP	RU-14	
AD8574ARUZ	−40°C to +125°C	14-Lead TSSOP	RU-14	
AD8574ARUZ-REEL	−40°C to +125°C	14-Lead TSSOP	RU-14	

¹ Z = RoHS Compliant Part, # denotes RoHS compliant product may be top or bottom marked.

NOTES

NOTES

NOTES